Constraining the 3 – 3 – 1 model with heavy neutral leptons using $(g-2)_\mu$ and dark matter observables

C. E. Alvarez-Salazar[1,2,*] and O. L. G. Peres[2,†]

[1]*Laboratorio de Física, Universidad Manuela Beltrán, Avenida Circunvalar No. 60-00, 110231, Bogotá D.C., Colombia*

[2]*Instituto de Física Gleb Wataghin-UNICAMP, 13083-859 Campinas/SP, Brazil*

(Received 19 September 2019; accepted 1 February 2021; published 25 February 2021)

Models with gauge symmetry $SU(3)_c \otimes SU(3)_L \otimes U(1)_N$ have different candidates for dark matter, for example, a heavy neutral fermion interacting with standard model particles through different mediators, scalar and vector portals. At the same time, these portals can produce signals in the anomalous magnetic moment of the muon that violate the present bounds on this quantity. Combining the requirement to have a dark matter candidate in the $SU(3)_c \otimes SU(3)_L \otimes U(1)_N$ model with heavy neutral leptons and to explain the anomalous magnetic moment of the muon we set constraints on the highest symmetry breaking scale of the model. These bounds are competitive with the constraints from LHC and set a favored region that can also be tested in future direct detection experiments, such as the LUX-ZEPLIN (LZ) experiment.

DOI: 10.1103/PhysRevD.103.035029

I. INTRODUCTION

Different experimental results point to the incompleteness of the standard model (SM) of particle physics as a theory describing the constituents of nature. The observation of neutrino oscillations, explained only in the framework of massive neutrinos [1], the discrepancy between the SM prediction with the measured value of the anomalous magnetic moment of the muon [2], the baryon asymmetry of the Universe [3], and the conclusion that only 5% of the energy content of the Universe is constituted by particles in the SM [4], are some strong indications that physics beyond the SM is needed.

The inclusion of matter with no interaction with light, explaining the reason to be called dark matter (DM), as a fundamental component of the theoretical model of particle physics, has been considered mandatory in the last years due to different observations, both at galactic and cosmological scales [5,6]. Several results have led to the conclusion that 27% of the energy in the Universe corresponds to matter in a form not included in the SM [7].

Due to the unknown nature of DM, it is important to construct theoretical frameworks to describe its interactions with SM particles, and this could have different degrees of refinement.

In the first place, the description of DM interactions in terms of effective field theories (EFT) constitutes a natural tool to perform model-independent analyses in terms of four-field operators for the interactions of DM with nucleons [8], in the nonrelativistic limit. One advantage of this treatment is the possibility to obtain stringent bounds on the physics scale suppressing higher dimensional operators [9].

The second possibility for a theory of DM-SM interactions includes the most important mediator states, leading to a better description of the kinematics of the interaction. This step forward is done in the so-called simplified models [10,11], where the interactions can be described in scalar or vector channels for DM particles of any spin. This treatment has been proved useful in the search for new physics, where the interactions of a small number of new particles give predictions for collider physics observables at the Large Hadron Collider (LHC) [12].

Finally, complete models not only include DM particles and the mediators of their interactions in their particle contents, but (sometimes) a plethora of new particles. These models could be considered extensions of the SM, and are inspired by the most diverse ideas [13,14]. Usually, these models are set to solve or explain issues of the SM, what leads to the appearance of particles with the required characteristics to be identified with DM.

In this work, we analyze a $SU(3)_c \otimes SU(3)_L \otimes U(1)_N$ framework ($3-3-1$ model, for short) with heavy neutral fermions, in order to find constraints on the scale of $SU(3)_L$ symmetry breaking, which determines the mass scale of

*carlos.alvarez@docentes.umb.edu.co
†orlando@ifi.unicamp.br

new particles in the model, using the measured values of the anomalous magnetic moment of the muon [15], the DM relic density [7] and the exclusion limits set by DM direct detection experiments [16,17], when the candidate to DM in the model is one of the heavy neutral fermions.

In order to do this, we analyze all possible contributions to the anomalous magnetic moment of the muon, taking into account the calculation of the physical scalar states that appear in the model, as calculated in [18], and which gives new contributions due to the exchange of scalar particles, when compared with the previous analysis performed in [19] (using the physical scalars found in [20] based on an approximation for the eigenstates of 3×3 matrices), considering the contribution of only one of the neutral scalars in the physical spectrum of the model. Our method for calculating the neutral eigenstates induces a different phenomenology for the physical scalars as, for example, new interactions with leptons. This produces, as we will show later, two new contributions to the anomalous magnetic moment of the muon, not considered in the analysis performed in Ref. [19].

We also make a comparison of the complete $3-3-1$ framework with simplified models, determining the dominant channel for the interactions from the identification of resonances leading to the relic abundance of the fermion candidate to DM. This dominant channel turns out to be the exchange of a heavy gauge boson in the model. After this, we analyze the constraints on a simplified $3-3-1$ model with the fermion candidate to DM and the new gauge boson as the mediator of its interactions with SM particles, coming from direct detection experiments [16,17]. The analysis of minimal models for DM-SM interactions has been performed, for example, in [21], with fermions and scalars as additional fields, with no additional gauge boson in the models. On the other hand, the analysis of [22,23] includes different collider and DM direct detection constraints in the framework of simplified models for DM, and the calculation of contributions of new particles to the muon anomalous magnetic moment, introducing new scalars or fermions that can be in different representations of the SM gauge group. Our approach is different from this, in the sense that we determine first the dominant portal for the interactions in the $3-3-1$ model, and then analyze the results in the framework of a simplified model with a gauge boson as the mediator of DM-SM interactions, without including new scalar or fermion fields besides the DM candidate.

This paper is organized as follows. In Sec. II we will discuss briefly some motivations and characteristics of models beyond the SM, emphasizing on simplified models for the description of DM-SM interactions. In Sec. III we present a summary of the $3-3-1$ model considered in this work, in order to find, in Sec. IV, the contribution of new particles to the anomalous magnetic moment of the muon and, in Sec. V, the dominant portal for DM-SM interactions. Furthermore, in Sec. VI we find constraints on the mass of the mediator of DM-SM interactions, which can be translated in lower bounds for the $SU(3)_L$ symmetry breaking scale, and compare these results with the favored window coming from the contributions to the anomalous magnetic moment of the muon. Finally, in Sec. VII, we make a comparison of our results with previous constraints found on the $3-3-1$ model, mainly based on LHC data, and present our conclusions in Sec. VIII.

II. SIMPLIFIED MODELS FOR THE DESCRIPTION OF DM-SM INTERACTIONS

Models going beyond the SM try to solve some of its problems or inconsistencies leading to different frameworks with its own structure [24]. For example, in order to solve the gauge symmetry problem, associated with the chirality of electroweak interactions and the quantization of electric charge, a unification of interactions or a grand unified theory have been proposed [25,26]; for the solution of the fermion problem, related to the existence of at least three lepton families with hierarchical masses, superstring theories [27] or braneworld scenarios [28] can give an explanation; the hierarchy problem, associated with divergent corrections to the Higgs boson mass, can be solved, for example, in the framework of supersymmetry [29], extended models [30,31], dynamical mechanisms for symmetry breaking [32] or large extra dimensions [33,34].

Disregarding the details of any of these models, it is very desirable to have the possibility of embedding DM in their particle contents, which will interact with SM particles depending on the Lagrangian of the model. These interactions are completely unknown at the moment, and can be described in terms of simplified models, where the mediator state is called "portal" [9,10].

For models with a single candidate to DM, where a discrete symmetry protects the lightest odd particle of decaying, its interactions will depend on the particle types of the DM and the mediator. For example, in the case of fermionic DM, different from its own antiparticle and represented by a field ψ interacting with SM particles through a scalar S or vector U portal, the interaction Lagrangian can be written, respectively, as [11]

$$\mathcal{L} = g_\psi \bar{\psi}\psi S + \sum_f \frac{c_S m_f}{\sqrt{2} v_h} \bar{f} f S, \tag{1}$$

$$\mathcal{L} = g\bar{\psi}\gamma^\alpha (V_\psi^U - A_\psi^U \gamma_5)\psi U_\alpha + g\sum_f \bar{f}\,\gamma^\alpha (V_f^U - A_f^U \gamma_5) f U_\alpha, \tag{2}$$

where g_ψ and g are couplings associated with the interaction of ψ with S and U, respectively, c_S is a Yukawa-like coupling associated with the mass m_f of the SM fermions f, v_h is the vacuum expectation value of the Higgs boson,

and V_ψ^U, A_ψ^U (V_f^U, A_f^U) are vector and axial couplings of fermionic DM (SM) particles.

In order to identify DM particles, several direct and indirect experiments have been performed, are in progress or under construction. In the case of indirect searches, the detection of the decay or annihilation products of DM particles is used as a probe for DM particles [35,36]. On the other hand, in direct detection experiments the scattering of DM particles could leave a signal in the detectors, which can be in the form of energy deposition, scintillation light or ionization [37]. A fundamental quantity in direct detection experiments is the spin-independent scattering cross section of a DM candidate with nucleons, which is usually obtained in these experiments and which gives the strongest constraints on DM observables.

Using the interaction Lagrangian in Eqs. (1) and (2), this spin-independent scattering cross section with protons, σ_p^{SI}, for the cases of scalar and vector portals, is given by [38]

$$\sigma_p^{\mathrm{SI}} = \begin{cases} \frac{\mu_{\psi p}^2}{\pi} g_\psi^2 c_S^2 \frac{m_p^2}{v_h^2} \frac{f_N^2}{m_S^4} & \text{scalar portal,} \\ \frac{\mu_{\psi p}^2}{\pi} \frac{g^4}{m_U^4} \left(\frac{Z f_p + (A-Z) f_n}{A} \right)^2 & \text{vector portal,} \end{cases} \tag{3}$$

where $\mu_{\psi p}$ is the reduced mass of the fermion DM-proton system, with masses m_ψ and m_p, respectively, f_N ($N = n, p$) is the effective coupling of DM with nucleons, m_S and m_U are the masses of the scalar and vector mediators, and the atomic and mass numbers of the target in a direct detection experiment are denoted by Z and A, respectively.

III. THE 3 − 3 − 1 MODEL WITH HEAVY NEUTRAL LEPTONS

In this section we present a review of a complete model beyond the SM, for which a fermion DM candidate is contained in its particle spectrum, and for which we will calculate the contribution of new particles to the anomalous magnetic moment of the muon, and results on DM observables will be compared in terms of the simplified model predictions just discussed.

This extension corresponds to a model with gauge symmetry $SU(3)_c \otimes SU(3)_L \otimes U(1)_N$, initially proposed in [39–41], and which has been widely studied in the literature [42–44], due to its appealing characteristics. For example, the anomaly cancellation occurs only if the number of families is exactly three or one of its multiples [45], the quantization of electric charge appears naturally [46], neutrino masses can be included easily in the model, either by effective operators invariant under the gauge symmetry [47] or by a double see-saw mechanism [48], the strong CP problem can be solved and a nonthermal candidate for DM (an axion) can be included in its physical spectrum [48–51], and the model is very interesting from the phenomenological point of view [52].

In this $3-3-1$ model, it is customary to define the electric charge operator as a linear combination of the diagonal generators (T_i, I) of the group $SU(3)_L \otimes U(1)_N$ as $Q = T_3 + \beta T_8 + NI$, where β is an embedding parameter which determines the $U(1)_N$ quantum numbers and electric charges of new particles.

Despite the multiple versions of $3-3-1$ models existing in the literature, in this work we will analyze a version which does not contain exotic quark charges, characterized by a parameter $\beta = 1/\sqrt{3}$ [53], and containing heavy neutral fermions in the lepton triplets. The reason for choosing this model in comparison with other versions lies on the fact that this model contains scalar, fermionic, and vector DM candidates, but only the lightest of these particles can be considered a DM candidate, since all belong to the same discrete symmetry group used to stabilize DM [20]. This discrete symmetry will be presented after the introduction of the expression for the Yukawa Lagrangian, when all the field contents of the model have been introduced.

In order to cancel gauge anomalies, we distribute the matter content of the model in the following way [54]: the first two generations of left-handed quarks transform as triplets, while the third generation transforms as an antitriplet, in the same way as left-handed leptons:

$$\begin{aligned} q_{iL} &= (u_i, d_i, J_i)_L^T \sim (3, 3, 0), \\ q_{3L} &= (d_3, -u_3, J_3)_L^T \sim (3, \bar{3}, 1/3), \\ F_{jL} &= (l_j, -\nu_j, E_j)_L^T \sim (1, \bar{3}, -1/3), \end{aligned} \tag{4}$$

with $i = 1, 2$ corresponding to the first and second quark generation, $j = e, \mu, \tau$ denoting the three lepton families, and $\sim$ is used to indicate the transformation properties under the symmetry group. Note that the model contains one new up quark (J_3) and two new down quarks ($J_{1,2}$), alongside with three heavy neutral leptons E_j.

Right-handed particles are singlets under $SU(3)_L$, with the following transformation rules:

$$\begin{aligned} &l_{jR} \sim (1, 1, -1), \qquad E_{jR} \sim (1, 1, 0) \quad \text{(leptons)}, \\ &u_{aR} \sim (3, 1, 2/3), \quad a = 1, \ldots, 4 \quad \text{(up quarks)}, \\ &d_{bR} \sim (3, 1, -1/3), \quad b = 1, \ldots, 5 \quad \text{(down quarks)}, \end{aligned} \tag{5}$$

where the usual quark generations correspond to $a, b = 1, \ldots, 3$.

Symmetry breaking in the model happens through three scalar triplets η, ρ, and χ, with the following components and transformation properties:

$$\eta = \begin{pmatrix} \eta^0 \\ \eta^- \\ \eta'^- \end{pmatrix} \sim \left(1, 3, -\frac{2}{3}\right), \qquad \rho = \begin{pmatrix} \rho^+ \\ \rho^0 \\ \rho'^0 \end{pmatrix} \sim \left(1, 3, \frac{1}{3}\right),$$
$$\chi = \begin{pmatrix} \chi^+ \\ \chi'^0 \\ \chi^0 \end{pmatrix} \sim \left(1, 3, \frac{1}{3}\right) \tag{6}$$

interacting through a scalar potential consistent with renormalization and gauge invariance, on which a discrete symmetry $\mathbb{Z}_2$ is imposed in order to bring simplicity to the model and interpret the χ scalar triplet as the one responsible for breaking the $SU(3)_L$ symmetry to the SM one,

$$\begin{aligned} V(\eta,\rho,\chi) = {} & \mu_1^2\eta^\dagger\eta + \mu_2^2\rho^\dagger\rho + \mu_3^2\chi^\dagger\chi \\ & + \lambda_1(\eta^\dagger\eta)^2 + \lambda_2(\rho^\dagger\rho)^2 + \lambda_3(\chi^\dagger\chi)^2 \\ & + \lambda_4(\chi^\dagger\chi)(\eta^\dagger\eta) + \lambda_5(\chi^\dagger\chi)(\rho^\dagger\rho) + \lambda_6(\eta^\dagger\eta)(\rho^\dagger\rho) \\ & + \lambda_7(\chi^\dagger\eta)(\eta^\dagger\chi) + \lambda_8(\chi^\dagger\rho)(\rho^\dagger\chi) + \lambda_9(\eta^\dagger\rho)(\rho^\dagger\eta) \\ & - \sqrt{2} f \epsilon_{ijk}\eta_i\rho_j\chi_k + \text{H.c.}, \end{aligned} \tag{7}$$

where μ_i $(i = 1, 2, 3)$ are quadratic self-interactions that can be determined from the vacuum properties, λ_i $(i = 1, \ldots, 9)$ are quartic couplings determining the spectrum of scalars in the theory, and f is a trilinear coupling usually taken proportional to the highest energy breaking scale in the model. The stability of this scalar potential was recently analyzed in [55], where tree-level constraints on the parameters of the model were obtained using copositivity conditions and current bounds on the masses of extra particles.

The Yukawa Lagrangian, responsible to give mass to quarks and leptons, is written as follows:

$$\mathcal{L}_Y = \mathcal{L}_Y^\eta + \mathcal{L}_Y^\rho + \mathcal{L}_Y^\chi, \tag{8}$$

where $\mathcal{L}_Y^\phi$ $(\phi = \eta, \rho, \chi)$ are the Yukawa terms corresponding to each of the scalar fields in Eq. (6), and given by [56]

$$\begin{aligned} -\mathcal{L}_Y^\eta &= \alpha_{ij}\overline{q_{iL}}\eta u_{jR} + \beta_{3j}\overline{q_{3L}}\eta^* d_{jR} + \gamma_{jk}\overline{l_{jL}}\eta^* e_{kR} + \text{H.c.} \\ -\mathcal{L}_Y^\rho &= \alpha_{3j}\overline{q_{3L}}\rho^* u_{jR} + \beta_{ij}\overline{q_{iL}}\rho d_{jR} + \text{H.c.} \\ -\mathcal{L}_Y^\chi &= \beta_{ib}\overline{q_{iL}}\chi d_{bR} + \alpha_{34}\overline{q_{3L}}\chi^* u_{4R} + \gamma'_{jk}\overline{l_{jL}}\chi^* E_{kR} \\ &\quad + \text{H.c.}, \end{aligned} \tag{9}$$

where different indices run as follows: $i = 1, 2$, $j, k = 1, \ldots, 3$, $b = 4, 5$.

The scalar triplets in Eq. (6) are responsible to give mass to all particles in the model. For example, physical scalars appear as the massive eigenstates of the mass matrices obtained when the scalar triplets get the vacuum expectation values (VEVs)

$$\langle\eta\rangle = \frac{1}{\sqrt{2}}\begin{pmatrix} v_\eta \\ 0 \\ 0 \end{pmatrix}, \quad \langle\rho\rangle = \frac{1}{\sqrt{2}}\begin{pmatrix} 0 \\ v_\rho \\ 0 \end{pmatrix}, \quad \langle\chi\rangle = \frac{1}{\sqrt{2}}\begin{pmatrix} 0 \\ 0 \\ v_\chi \end{pmatrix}, \tag{10}$$

and the components η^0, ρ^0, and χ^0 are decomposed into their real $(R_{\eta,\rho,\chi})$ and imaginary $(I_{\eta,\rho,\chi})$ parts,

$$\begin{aligned} \eta^0 &= \frac{1}{\sqrt{2}}(R_\eta + iI_\eta), \qquad \rho^0 = \frac{1}{\sqrt{2}}(R_\rho + iI_\rho), \\ \chi^0 &= \frac{1}{\sqrt{2}}(R_\chi + iI_\chi), \end{aligned} \tag{11}$$

leading to the mass matrices

$$\mathcal{M}_R^2 = \begin{pmatrix} 2\lambda_1 v_\eta^2 + \frac{f v_\rho v_\chi}{v_\eta} & \lambda_6 v_\eta v_\rho - f v_\chi & \lambda_4 v_\eta v_\chi - f v_\rho \\ \lambda_6 v_\eta v_\rho - f v_\chi & 2\lambda_2 v_\rho^2 + \frac{f v_\eta v_\chi}{v_\rho} & \lambda_5 v_\rho v_\chi - f v_\eta \\ \lambda_4 v_\eta v_\chi - f v_\rho & \lambda_5 v_\rho v_\chi - f v_\eta & 2\lambda_3 v_\chi^2 + \frac{f v_\eta v_\rho}{v_\chi} \end{pmatrix}, \tag{12}$$

$$\mathcal{M}_I^2 = \begin{pmatrix} \frac{f v_\eta v_\chi}{v_\rho} & f v_\chi & f v_\eta \\ f v_\chi & \frac{f v_\rho v_\chi}{v_\eta} & f v_\rho \\ f v_\eta & f v_\rho & \frac{f v_\eta v_\rho}{v_\chi} \end{pmatrix}. \tag{13}$$

The calculation of eigenvectors and eigenvalues of the first of these matrices leads to three physical states h, H_2, and H_3 and their corresponding masses.[1] Under special assumptions on the entries of the mass matrix (12), trying to reduce $\mathcal{M}_R^2$ to a block-diagonal form, the physical states have been calculated in [19,20]. Under these simplifying assumptions, the scalar H_3 is identified with the real part R_χ of the third component of the χ scalar triplet, with no R_η or R_ρ components. In the same way, the physical scalars h and H_2 lack a component proportional to R_χ. In this way, the substitution of the symmetry states in terms of the physical states in the Lagrangian of the model lacks interactions between the scalars h, H_2, and H_3 with other particles in the model, appearing from the Yukawa terms in Eq. (9), and which will give sizeable contributions to physical observables as, for example, the muon anomalous magnetic moment, as will be seen in Sec. IV. So, it is important to keep all entries in Eq. (12) for the calculation of the physical states h, H_2, and H_3, which will depend on the three real components R_η, R_ρ, and R_χ, in such a way that all interactions of the physical states are taken into account.

[1]We identify the lightest physical state h with the SM Higgs boson.

To get a more precise calculation of the physical scalars and their interactions in the model, we have kept the full matrix (12) and calculated its eigenvectors and eigenvalues using the Rayleigh-Schrödinger perturbation theory [57,58], in the same way as in Ref. [18], but including the second-order correction to the eigenvectors. To use this formalism, we write (12) as an analytic perturbation [in the dimensionless parameter $\frac{v}{v_\chi}$, where $v^2 = v_\eta^2 + v_\rho^2 = (246\ \mathrm{GeV})^2$] of a matrix for which eigenvectors and eigenvalues are easily calculated. More specifically, we write (12) as

$$\mathcal{M}_R^2 = v_\chi^2\left[\mathcal{A}_0 + \frac{v}{v_\chi}\mathcal{A}_1 + \left(\frac{v}{v_\chi}\right)^2\mathcal{A}_2\right], \tag{14}$$

where $\mathcal{A}_0$, $\mathcal{A}_1$, and $\mathcal{A}_2$ are the nonperturbed, first- and second-order perturbations, respectively, given by the following expressions:

$$\mathcal{A}_0 = \begin{pmatrix} \frac{kv_\rho}{v_\eta} & -k & 0 \\ -k & \frac{kv_\eta}{v_\rho} & 0 \\ 0 & 0 & 2\lambda_3 \end{pmatrix}, \tag{15}$$

$$\mathcal{A}_1 = \begin{pmatrix} 0 & 0 & \frac{\lambda_4 v_\eta}{v} - \frac{kv_\rho}{v} \\ 0 & 0 & \frac{\lambda_5 v_\rho}{v} - \frac{kv_\eta}{v} \\ \frac{\lambda_4 v_\eta}{v} - \frac{kv_\rho}{v} & \frac{\lambda_5 v_\rho}{v} - \frac{kv_\eta}{v} & 0 \end{pmatrix}, \tag{16}$$

$$\mathcal{A}_2 = \begin{pmatrix} 2\lambda_1\left(\frac{v_\eta}{v}\right)^2 & \frac{\lambda_6 v_\eta v_\rho}{v^2} & 0 \\ \frac{\lambda_6 v_\eta v_\rho}{v^2} & 2\lambda_2\left(\frac{v_\rho}{v}\right)^2 & 0 \\ 0 & 0 & \frac{kv_\eta v_\rho}{2v^2} \end{pmatrix}, \tag{17}$$

where we have made the substitution $f = kv_\chi$ for the trilinear coupling in the scalar potential (7), in order to avoid the introduction of a new energy scale.

The unperturbed masses of the physical fields h, H_2, and H_3 are obtained as the product of the eigenvalues of the matrix $\mathcal{A}_0$ and v_χ^2, and are given by

$$\begin{aligned} (M_h^{(0)})^2 &= 0, \\ (M_{H_2}^{(0)})^2 &= \frac{kv^2}{2v_\eta v_\rho}v_\chi^2, \\ (M_{H_3}^{(0)})^2 &= 2\lambda_3 v_\chi^2, \end{aligned} \tag{18}$$

and the physical fields, to the same order, are

$$\begin{aligned} h^{(0)} &= \frac{v_\eta}{v}R_\eta + \frac{v_\rho}{v}R_\rho, \\ H_2^{(0)} &= -\frac{v_\rho}{v}R_\eta + \frac{v_\eta}{v}R_\rho, \\ H_3^{(0)} &= R_\chi. \end{aligned} \tag{19}$$

The first-order perturbation $\mathcal{A}_1$ gives no correction to the masses in Eq. (18), but induces the following correction to the physical fields:

$$\begin{aligned} h^{(1)} &= -\frac{\lambda_4 v_\eta^2 - 2kv_\eta v_\rho + \lambda_5 v_\rho^2}{2\lambda_3 v v_\chi}R_\chi, \\ H_2^{(1)} &= \frac{v_\eta v_\rho[k(v_\rho^2 - v_\eta^2) + (\lambda_5 - \lambda_4)v_\eta v_\rho]}{v v_\chi(kv^2 - 2\lambda_3 v_\eta v_\rho)}R_\chi, \\ H_3^{(1)} &= \frac{v_\eta[k(\lambda_4 v_\eta^2 + (2\lambda_3 + \lambda_5)v_\rho^2) - 2v_\eta v_\rho(k^2 + \lambda_3\lambda_4)]}{2\lambda_3 v_\chi(kv^2 - 2\lambda_3 v_\eta v_\rho)}R_\eta \\ &\quad + \frac{v_\rho[k(\lambda_5 v_\rho^2 + (2\lambda_3 + \lambda_4)v_\eta^2) - 2v_\eta v_\rho(k^2 + \lambda_3\lambda_5)]}{2\lambda_3 v_\chi(kv^2 - 2\lambda_3 v_\eta v_\rho)}R_\rho. \end{aligned} \tag{20}$$

The matrix $\mathcal{A}_2$ induces the following correction to the masses of the physical fields:

$$\begin{aligned} (M_h^{(2)})^2 &= \frac{(4\lambda_1\lambda_3 - \lambda_4^2)v_\eta^4 + 4k(\lambda_4 v_\eta^3 v_\rho + \lambda_5 v_\eta v_\rho^3) - 2(2k^2 + \lambda_4\lambda_5 - 2\lambda_3\lambda_6)v_\eta^2 v_\rho^2 + (4\lambda_2\lambda_3 - \lambda_5^2)v_\rho^4}{2\lambda_3 v^2}, \\ (M_{H_2}^{(2)})^2 &= \frac{v_\eta v_\rho[(k(v_\eta^2 - v_\rho^2) + (\lambda_4 - \lambda_5)v_\eta v_\rho)^2 + 2v_\eta v_\rho(\lambda_1 + \lambda_2 - \lambda_6)(kv^2 - 2\lambda_3 v_\eta v_\rho)]}{v^2(kv^2 - 2\lambda_3 v_\eta v_\rho)}, \\ (M_{H_3}^{(2)})^2 &= \frac{k(\lambda_4 v_\eta^2 + \lambda_5 v_\rho^2)[(\lambda_4 v_\eta^2 + \lambda_5 v_\rho^2) - 4kv_\eta v_\rho] - 4kv_\eta^2 v_\rho^2[k^2 + \lambda_3(\lambda_3 - \lambda_4 - \lambda_5)] - 2\lambda_3 v_\eta v_\rho(\lambda_4^2 v_\eta^2 + \lambda_5^2 v_\rho^2)}{2\lambda_3(kv^2 - 2\lambda_3 v_\eta v_\rho)}, \end{aligned} \tag{21}$$

and the second-order perturbation to the physical states given by

$$h^{(2)} = F_1(\lambda, k, v_\eta, v_\rho, v_\chi)(v_\rho R_\eta - v_\eta R_\rho),$$
$$H_2^{(2)} = F_2(\lambda, k, v_\eta, v_\rho, v_\chi)(v_\eta R_\eta + v_\rho R_\rho),$$
$$H_3^{(2)} = 0, \tag{22}$$

where the functions $F_{1,2}(\lambda, k, v_\eta, v_\rho, v_\chi)$ are given by

$$F_1(\lambda, k, v_\eta, v_\rho, v_\chi) = \frac{v_\eta v_\rho}{2k\lambda_3 v^5 v_\chi^2}[v_\eta^3 v_\rho(\lambda_4(\lambda_4-\lambda_5)+2\lambda_3(\lambda_6-2\lambda_1))+2k^2 v_\eta v_\rho(v_\rho^2-v_\eta^2)$$
$$+ v_\eta v_\rho^3(\lambda_5(\lambda_4-\lambda_5)+2\lambda_3(2\lambda_2-\lambda_6))+k(\lambda_4 v_\eta^4+3v_\eta^2 v_\rho^2(\lambda_5-\lambda_4)-\lambda_5 v_\rho^4)] \tag{23}$$

and

$$F_2(\lambda, k, v_\eta, v_\rho, v_\chi) = \frac{v_\eta^2 v_\rho^2}{kv^5(kv^2-2\lambda_3 v_\eta v_\rho)v_\chi^2}[v_\eta^3 v_\rho(\lambda_4(\lambda_5-\lambda_4)+2\lambda_3(2\lambda_1-\lambda_6))-2k^2 v_\eta v_\rho(v_\rho^2-v_\eta^2)$$
$$+ v_\eta v_\rho^3(\lambda_5(\lambda_5-\lambda_4)+2\lambda_3(\lambda_6-2\lambda_2))+kv_\eta^4(\lambda_6-\lambda_4-2\lambda_1)+kv_\eta^2 v_\rho^2(2(\lambda_2-\lambda_1)+3(\lambda_4-\lambda_5))$$
$$- kv_\rho^4(\lambda_6-\lambda_5-2\lambda_2)]. \tag{24}$$

Using these results, we can write the transformation between the physical states h, H_2, and H_3 and the symmetry states R_η, R_ρ, and R_χ as

$$\begin{pmatrix} h \\ H_2 \\ H_3 \end{pmatrix} = \begin{pmatrix} U_{1,1}^H & U_{1,2}^H & U_{1,3}^H \\ U_{2,1}^H & U_{2,2}^H & U_{2,3}^H \\ U_{3,1}^H & U_{3,2}^H & U_{3,3}^H \end{pmatrix} \begin{pmatrix} R_\eta \\ R_\rho \\ R_\chi \end{pmatrix}, \tag{25}$$

where the expressions for the components of the transformation matrix $U_{i,j}^H$ can be read from Eqs. (19), (20), and (22).

On the other hand, matrix (13) gives a pseudoscalar particle H_0, with a mass

$$M_{H_0}^2 = \frac{k(v_\eta^2 v_\rho^2 + v^2 v_\chi^2)}{v_\eta v_\rho}, \tag{26}$$

and two Goldstone bosons G_Z and $G_{Z'}$, eaten by the neutral gauge bosons appearing in the physical spectrum, to be discussed later. The transformation between these states and the imaginary components I_η, I_ρ, and I_χ is given by

$$\begin{pmatrix} H_0 \\ G_Z \\ G_{Z'} \end{pmatrix} = \begin{pmatrix} U_{1,1}^h & U_{1,2}^h & U_{1,3}^h \\ U_{2,1}^h & U_{2,2}^h & U_{2,3}^h \\ U_{3,1}^h & U_{3,2}^h & U_{3,3}^h \end{pmatrix} \begin{pmatrix} I_\eta \\ I_\rho \\ I_\chi \end{pmatrix}$$
$$= \begin{pmatrix} -\frac{v_\rho}{\sqrt{v_\rho^2+v_\chi^2}} & 0 & \frac{v_\chi}{\sqrt{v_\rho^2+v_\chi^2}} \\ -\frac{v_\rho}{\sqrt{v_\eta^2+v_\rho^2}} & \frac{v_\eta}{\sqrt{v_\eta^2+v_\rho^2}} & 0 \\ \frac{1}{v_\rho\sqrt{\frac{1}{v_\eta^2}+\frac{1}{v_\rho^2}+\frac{1}{v_\chi^2}}} & \frac{1}{v_\eta\sqrt{\frac{1}{v_\eta^2}+\frac{1}{v_\rho^2}+\frac{1}{v_\chi^2}}} & \frac{1}{v_\chi\sqrt{\frac{1}{v_\eta^2}+\frac{1}{v_\rho^2}+\frac{1}{v_\chi^2}}} \end{pmatrix} \begin{pmatrix} I_\eta \\ I_\rho \\ I_\chi \end{pmatrix}. \tag{27}$$

To complete the spectrum of scalar states in the theory, the mass mixing matrices resulting from the charged symmetry states in (6) give two bosons, labeled $H_W^\pm$ and $H_Y^\pm$, and the neutral states without a VEV in the same equation give an additional neutral scalar H_V which can be another possible candidate to DM in the model, stabilized by the same discrete symmetry than the heavy neutral fermion E_e.

The gauge sector of the model consists, besides the SM photon A and the mediators of weak interactions $W^\pm$ and Z, on a new charged gauge boson $Y^\pm$ and two additional neutral fields V^0 and Z'. The first of these neutral fields can also be made a DM candidate in the model (under the same symmetry used to stabilize the heavy neutral fermion E_e and the neutral gauge boson H_V), and the second of these gauge fields appears from the 3×3 mixing matrix of neutral gauge bosons, from which A and Z correspond to the other two eigenstates.

For paramount importance for this work, the lightest of the heavy neutral fermions in Eq. (4) can be made a DM candidate in the model using a residual global symmetry $U(1)_G$ [20] appearing after the electroweak symmetry breaking, with the following charge assignments

$$G(E_j, J_3, \bar{J}_{1,2}, Y^-, V^0, \eta^-, \rho'^0, \chi'^0, \chi^-) = -1, \tag{28}$$

which implies the existence of five neutral odd particles: the three heavy neutral leptons E_j ($j = e, \mu, \tau$), the scalar H_V, and the gauge boson V^0. The lightest of these particles can be identified as a DM particle stabilized by this symmetry, and we will analyze the DM observables associated with the heavy neutral lepton of the electron flavor in Secs. V and VI.

In the following section we will find the contribution of new particles in this $3-3-1$ model to the anomalous

magnetic moment of the muon, in order to determine if the physical spectrum can give a sizeable deviation of the SM prediction of this precisely measured quantity, which can be used as a sensitive probe for models beyond SM.

IV. CONSTRAINTS FROM THE MUON ANOMALOUS MAGNETIC MOMENT

In order to set constraints on the scale of symmetry breaking of the $SU(3)_L$ group, we have used the computation of the contribution of new particles in the $3-3-1$ model to the anomalous magnetic moment of the muon, defined as

$$a_\mu = \frac{g_\mu - 2}{2}, \tag{29}$$

where g_μ is the gyromagnetic ratio (or g-factor), in terms of which the orbital magnetic moment of the muon is written in terms of its spin $\vec{S}$ as

$$\vec{\mu} = -g_\mu \mu_0 \vec{S}, \tag{30}$$

where μ_0 is the Bohr magneton. The usefulness of this comparison lies on the fact that $\Delta a_\mu \equiv a_\mu^{\rm exp} - a_\mu^{\rm SM}$, where $a_\mu^{\rm exp}$ is the experimentally measured value and $a_\mu^{\rm SM}$ the SM prediction, is a quantity measured very precisely in particle physics [15], and which can be used in order to set constraints on models beyond the SM [59].

In order to calculate the contribution of new particles in the spectrum of the $3-3-1$ model considered in this work, we need to identify the possible one-loop lowest order type diagrams taking into account the exchange of both neutral and charged bosons. The contributing diagrams are shown in Fig. 1, and the general expressions for Δa_μ associated with diagrams of this kind can be found in [2]. A very complete calculation which also includes a numerical code is available in Ref. [60].

The contribution of the exchange of neutral scalar particles H_2, H_3, and H_0 [Fig. 1(a)] has the form

$$\Delta a_\mu^S = \frac{f_S^2}{8\pi^2}\lambda_S^2 \int_0^1 dx \frac{x^2(2-x)}{1-x+\lambda_S^2 x^2}, \tag{31}$$

with $S = H_2, H_3, H_0$ a label indicating the particle exchanged (with mass M_S), and $\lambda_S = m_\mu/M_S$, with m_μ the muon mass.

In Eq. (31), f_S ($S = H_2, H_3, H_0$) represents the vertex factor associated with the $\{\mu^-, \mu^+, S\}$ interaction given by

$$f_{H_2} = \frac{U^H_{2,2} y_\mu}{\sqrt{2}}, \qquad f_{H_3} = \frac{U^H_{2,3} y_\mu}{\sqrt{2}}, \qquad f_{H_0} = \frac{U^h_{2,1} y_\mu}{\sqrt{2}}, \tag{32}$$

where $y_\mu = \frac{m_\mu \sqrt{2}}{v_\eta}$ is the diagonal Yukawa coupling of the muon, and $U^H_{i,j}$ and $U^h_{i,j}$ are the i, j elements of the transformation matrices (25) and (27), respectively. It is important to note here that the nonvanishing components $U^H_{2,3}$ and $U^h_{2,1}$ of the transformation matrices in Eqs. (25) and (27) induce two new contributions to the anomalous magnetic moment of the muon when compared with the previous calculation performed in Ref. [19], namely, the ones coming from the interchange of the real scalar H_3 and the pseudoscalar H_0. The numerical calculation of the contribution of the exchange of neutral scalar particles (which can be seen in Fig. 2) has shown that the one due to the scalar H_3 is the most important one, as this contribution lies in the experimentally measured interval for Δa_μ.

The contribution of the diagram where a Z' boson is exchanged [see Fig. 1(b)] has two contributions, due to the vector and axial couplings of this boson to the muon [62], and is given by

$$\Delta a_\mu^{Z'} = \frac{\lambda_{Z'}^2}{4\pi^2}\left[(V_\mu^{Z'})^2 \int_0^1 dx \frac{x^2(1-x)}{1-x+\lambda_{Z'}^2 x^2} + (A_\mu^{Z'})^2 \int_0^1 dx \frac{x(1-x)(x-4) - 2\lambda_{Z'}^2 x^3}{1-x+\lambda_{Z'}^2 x^2}\right], \tag{33}$$

where $V_\mu^{Z'}$ and $A_\mu^{Z'}$ are the vector and axial couplings of the Z' vector boson to the muon [using the same notation in Eq. (2)], and $\lambda_{Z'}$ is the ratio of the muon mass to the Z' mass. These quantities are defined as follows:

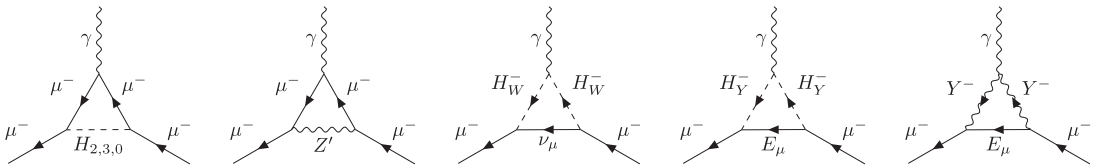

FIG. 1. Contributions to the anomalous magnetic moment of the muon in the $3-3-1$ model considered in this work, for different exchanged particles (a) H_2, H_3, or H_0 neutral bosons, (b) Z' gauge boson, (c) $H_W^\pm$, and (d) $H_Y^\pm$ charged scalar bosons, respectively, and (e) $Y^\pm$ charged vector boson.

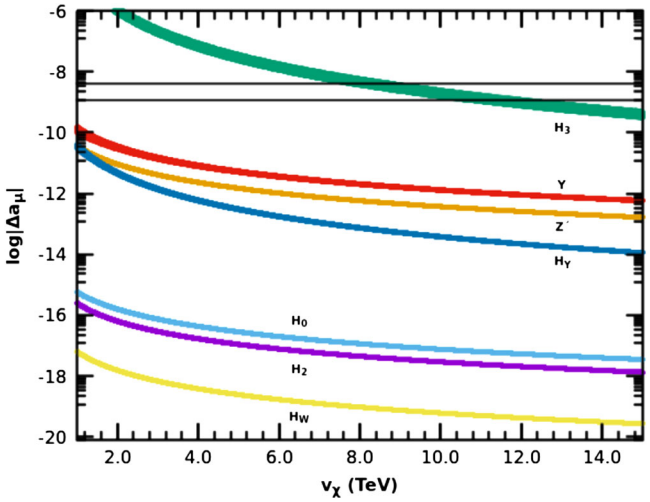

FIG. 2. Contributions to Δa_μ of new particles in the $3-3-1$ model considered in this work. The contributions of H_2, H_3, and $Y_\mu^\pm$ are positive, and the contribution of all other particles is negative. The horizontal black lines represent the current value of Δa_μ (95% C.L.) [61].

$$V_\mu^{Z'} = \frac{e(1-4s_W^2)}{c_W s_W \sqrt{3-4s_W^2}}, \qquad A_\mu^{Z'} = -\frac{1}{1-4s_W^2} f_{Z'}^V,$$
$$\lambda_{Z'} = \frac{m_\mu}{M_{Z'}} \tag{34}$$

where e is the electron charge, and s_W and c_W are the sine and cosine of the Weinberg angle, respectively.

Contributions from the exchange of the charged scalar $H_W^\pm$, shown in Fig. 1(c), are simpler than the others, due to the presence of the muon neutrino in the loop. In the limit $m_{\nu_\mu} \ll m_\mu$, the contribution is reduced to

$$\Delta a_\mu^{H_W} = -\frac{f_{H_W}^2 \lambda_{H_W}^2}{24\pi^2}, \tag{35}$$

where f_{H_W} is the $\{\mu^-, H_W^+, \nu_\mu\}$ vertex factor, given by

$$f_{H_W} = -\frac{m_\mu}{\sqrt{2(v_\eta^2+v_\rho^2)}} \quad \text{and} \quad \lambda_{H_W} = \frac{m_\mu}{M_{H_W}}. \tag{36}$$

The exchange of charged scalars $H_Y^\pm$ in Fig. 1(d) gives the following contribution to the anomalous magnetic moment of the muon

$$\Delta a_\mu^{H_Y} = -\frac{\lambda_{H_Y}^2}{8\pi^2}\left[(f_{H_Y}^S)^2 \int_0^1 dx \frac{x(1-x)(x+\epsilon_{H_Y})}{(\epsilon_{H_Y}\lambda_{H_Y})^2(1-x)(1-\epsilon_{H_Y}^{-2}x)+x} + (f_{H_Y}^P)^2 \int_0^1 dx \frac{x(1-x)(x-\epsilon_{H_Y})}{(\epsilon_{H_Y}\lambda_{H_Y})^2(1-x)(1-\epsilon_{H_Y}^{-2}x)+x}\right] \tag{37}$$

where the λ and ϵ parameters are

$$\lambda_{H_Y} = \frac{m_\mu}{M_{H_Y}} \quad \text{and} \quad \epsilon_{H_Y} = \frac{M_{E_\mu}}{m_\mu},$$

with M_{H_Y} and M_{E_μ} the $H_Y^\pm$ and E_μ masses, respectively, and $f_{H_Y}^{S,P}$ are the scalar (S) and pseudoscalar (P) couplings of the $\{\mu^-, H_Y^+, E_\mu\}$ vertex, given by

$$f_{H_Y}^S = -\frac{1}{\sqrt{2(v_\rho^2+v_\chi^2)}}\left[m_{E_\mu}\frac{v_\rho}{v_\chi} + m_\mu \frac{v_\chi}{v_\rho}\right],$$
$$f_{H_Y}^P = \frac{1}{\sqrt{2(v_\rho^2+v_\chi^2)}}\left[m_{E_\mu}\frac{v_\rho}{v_\chi} - m_\mu \frac{v_\chi}{v_\rho}\right]. \tag{38}$$

Finally, as the charged gauge boson $Y_\mu^\pm$ has vector and axial couplings (with the same strength) with μ and E_μ, its contribution to the anomalous magnetic moment of the muon, calculated from the diagram in Fig. 1(e), can be written as

$$\Delta a_\mu^Y = \frac{f_Y^2 \lambda_Y^2}{4\pi^2}\int_0^1 dx \frac{2x^2(1+x)+\lambda_Y^2 x(1-x)(x(1+\epsilon_Y^2)-2\epsilon_Y^2)}{(\epsilon_Y\lambda_Y)^2(1-x)(1-\epsilon_Y^{-2}x)+x}, \tag{39}$$

with

$$f_Y = \frac{e}{2\sqrt{2}s_W}, \qquad \lambda_Y = \frac{m_\mu}{M_Y}, \quad \text{and} \quad \epsilon_Y = \frac{M_{E_\mu}}{m_\mu}, \tag{40}$$

where M_Y is the mass of the $Y_\mu^\pm$ boson.

We have numerically calculated the contributions of all these new particles in the $3-3-1$ model [Eqs. (31) for H_2, H_3 and H_0, (33) for Z'_μ, (35) for $H_W^\pm$, (37) for $H_Y^\pm$, and (39) for $Y_\mu^\pm$] to the anomalous magnetic moment of the muon, and obtained the results shown in Fig. 2, where the contribution of each particle to Δa_μ is shown as a function of the $SU(3)_L$ symmetry breaking scale v_χ, on which the mass of each of these particles is strongly dependent. For the calculation of these contributions, we have kept all free parameters in the scalar potential (7) of order one, and assumed $v_\eta \approx v_\rho$.

It is important to note here that the contributions of the CP-even scalars H_2 and H_3, and of the charged gauge boson $Y_\mu^\pm$, are positive, but the contributions of the CP-odd scalar H_0, the neutral gauge boson Z'_μ, and the charged scalars $H_W^\pm$ and $H_Y^\pm$ are negative. Additionally, note the presence of two additional contributions to the anomalous magnetic moment of the muon, not considered in the previous calculation performed in [19], due to the exchange of the scalars H_3 and H_0, and appearing from the

determination of the mass eigenstates of the matrices (12) and (13) taking into account all their entries.

In order to make a comparison with the reported value of Δa_μ [61], we have included in Fig. 2 the boundaries for this quantity (at 95% C.L.), represented by horizontal black lines. It is clear from this graph that the dominant contribution comes from the CP-even scalar H_3, which is at least 2 orders of magnitude greater than other contributions. From this graph it is possible to see that the H_3 contribution lies in the interval experimentally measured for values of the $SU(3)_L$ symmetry breaking scale such that

$$7.2\ \text{TeV} \lesssim v_\chi \lesssim 12.2\ \text{TeV} \quad (95\%\ \text{C.L.}), \tag{41}$$

determining a favored window to look for the masses of the new particles present in the spectrum, as we will do in Sec. VI with the Z' boson.

An important remark before ending this section concerns the possible modification of the results in Fig. 2 and the constraint given by Eq. (41) when we take different values for the λ parameters in the scalar potential, which were initially taken of order one, as was said before. We have tested our results against the choice of parameters, and found that random values of the λ parameters in the scalar potential in Eq. (7) give results with deviations not greater than 5% from the ones presented here, when the $\rho-\chi$ coupling λ_5 in the scalar potential is of order one, which maximizes the $\mu - H_3$ coupling.

In the following section, we will discuss the results for DM observables in the $3-3-1$ model when we take the heavy neutral lepton of the electron flavor, E_e, as our DM candidate, identifying the dominant channel describing its interactions leading to a relic dark matter abundance consistent with the measurements performed by the Planck Collaboration [4], and making a comparison of the results found in the complete $3-3-1$ model with the predictions of the simplified models presented in Sec. II.

V. IDENTIFICATION OF THE DOMINANT PORTAL OF DM-SM INTERACTIONS

In order to make a comparison of DM observables in the $3-3-1$ framework with the predictions of minimal DM models, we need to find the terms in the Lagrangian with the structure presented in Eqs. (1) and (2). Taking a look at the full Lagrangian in the FeynRules [63,64] implementation of the $\beta = 1/\sqrt{3}$ version of the model [56] and using the CalcHEP [65] package, we have found that, in the case where the lightest odd particle under the discrete symmetry corresponds to the heavy neutral fermion of the electron flavor, E_e, this particle interacts with four scalars in the physical spectrum of the model, and with four gauge bosons, leading to a relic E_e abundance in both the s and t channels.

The physical scalars interacting with the heavy neutral fermion E_e are the eigenstates h, H_2, and H_3 of the real mass matrix (12), and the CP-odd state H_0 corresponding to the massive eigenstate of the imaginary mass matrix (13). The interactions of these scalars with E_e give a sizeable relic abundance in the s channel, as will be seen later.

On the other hand, the heavy neutral fermion E_e interacts with four vector particles in the model, the SM Z boson, its heavier partner Z', the charged gauge boson $Y^\pm$, and the neutral V^0. The processes leading to an E_e relic abundance due to interactions with $Y^\pm$ and V^0 are performed in the t channel, with vertex factors inversely proportional to the v_χ vacuum expectation value, leading to a contribution less than 1% of the total DM abundance, and for these reasons are disregarded in the relic abundance computation. So, the contribution from interactions with vector channels comes from the s-channel interactions with the Z and Z' gauge bosons. This new gauge boson has a mass depending directly on the $SU(3)_L$ symmetry breaking scale v_χ,

$$M^2_{Z'} = \frac{g_W^2}{3-4s_W^2}\left(\frac{v_\rho^2(c_W^2-s_W^2)^2}{4c_W^2} + \frac{v_\eta^2}{4c_W^2} + c_W^2 v_\chi^2\right), \tag{42}$$

where g_W is the $SU(3)_L$ coupling constant.

In this way, we have seen that our DM candidate has the possibility to interact with SM particles both through scalar (h, H_2, H_3, and H_0) and vector (Z and Z') channels, allowing us to identify the dominant portal describing the interactions of the heavy neutral fermion E_e, through the determination of resonances in the cross section for processes leading to the candidate abundance, $E_e\overline{E_e} \leftrightarrow \text{XY}$, as the ones shown in Fig. 3. It has been shown [66] that interactions of DM particles through SM portals, mediated by the Higgs particle h or the Z gauge boson are almost completely ruled out by current constraints, and, even though these interactions are present in the $3-3-1$ model with heavy neutral leptons, the couplings of E_e to these particles are strongly suppressed

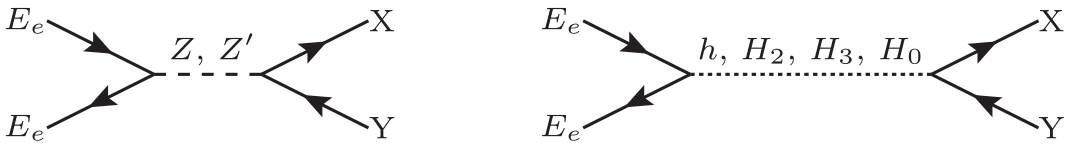

FIG. 3. s-channel diagrams for pair processes contributing to the relic abundance of E_e. The contribution of the t-channel processes involving $Y^\pm$ and V^0 is less than 1%.

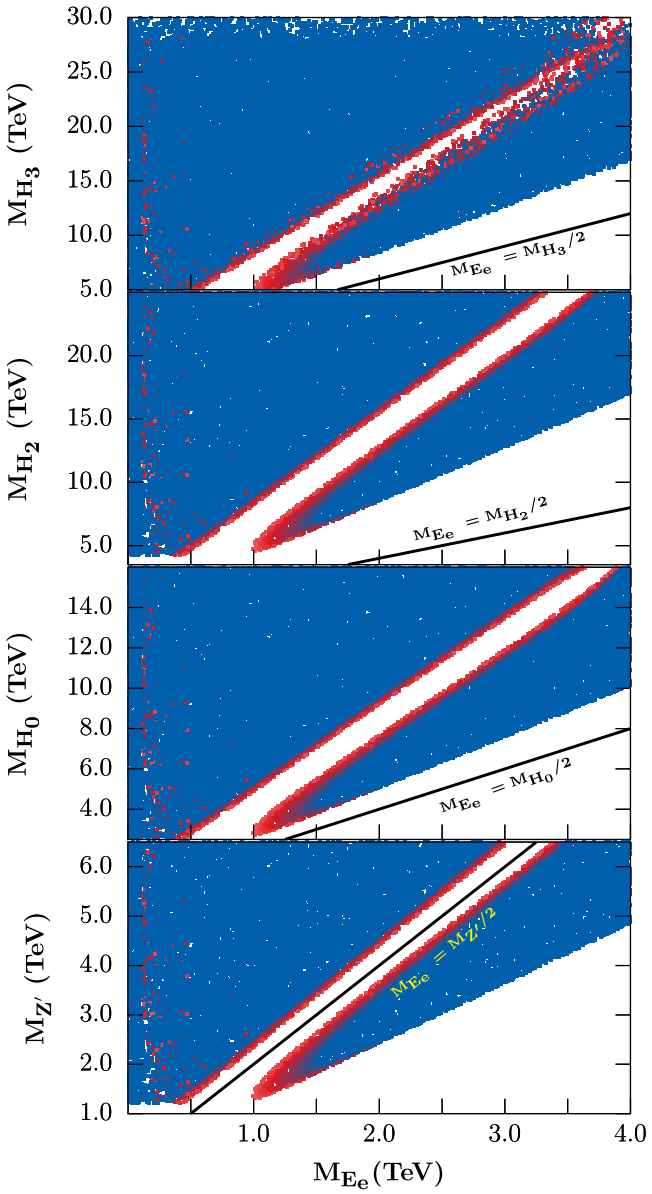

FIG. 4. Identification of the dominant portal for the interactions of a fermion E_e as candidate to DM in the $3-3-1$ model with heavy neutral leptons. Resonances on the relic abundance are determined by the position of the two red lines present in the figures: if the solid black line, described by $M_{E_e} = M_{\text{Mediator}}/2$, goes through the white stripe in the middle of the red lines giving a relic abundance consistent with Planck results [4], the dominant portal is characterized by the exchange of the corresponding mediator. The white regions in the lower right corners of each panel correspond to points on the parameter space where the lightest odd particle in the model is a charged gauge boson $Y^{\pm}$. The boundary between this region and the blue one corresponds to a degenerate regime where annihilations involving this boson enhance the heavy neutral lepton abundance.

by the highest energy scale v_χ, and for this reason are not included in our analysis.

Consequently, we have constructed the plots presented in Fig. 4, where we show a color map of the relic abundance of the heavy neutral fermion E_e in the plane M_{E_e} versus M_{Mediator}, where the color of each point indicates how the relic density Ω_{331} compares with the reported by the Planck Collaboration Ω_{Planck} [4]: blue points correspond to $\Omega_{331} > \Omega_{\text{Planck}}$, red points correspond to $\Omega_{331} \sim \Omega_{\text{Planck}}$, and the white dots in the middle of the two red lines in each diagram correspond to points where the relic density is below Ω_{Planck}. These graphs have been produced using the micrOMEGAs package [67], using a modified version of the FeynRules [63,64] implementation of the $3-3-1$ model in Ref. [56], including the calculation of the physical states h, H_2, and H_3 presented in Sec. III.

All plots in Fig. 4 were obtained when the coupling parameters in the scalar potential (7) are of order 1, $v_\eta \approx v_\rho$, and we guarantee that particles belonging to the same symmetry group that makes E_e stable have greater mass. Nevertheless, this is not always possible, as can be seen from the white region in the lower right corner of each panel in Fig. 4, which corresponds to points in the parameter space where E_e is no longer the lightest odd particle under the discrete symmetry, which is now substituted by the charged gauge boson $Y^{\pm}$. This degenerate scenario is reached when the heavy neutral fermion mass, M_{E_e}, is very close to the charged gauge boson mass, M_Y, and is observed in Fig. 4 as the boundary separating the blue region (with DM abundance greater than Ω_{Planck}) and the white region, where the lightest odd particle is now $Y^{\pm}$.

It is important to note here that, as the masses of E_e and $Y^{\pm}$ become closer, annihilation involving this particle can change drastically the heavy neutral lepton E_e relic abundance [68]. This degenerate regime is different to the general scenario depicted in Fig. 4, and its quantitative characteristics are not going to be described here, but our simulations for the scattering cross section with protons will give constraints for this regime. Another point that is worth mentioning is the appearance of some points with a relic abundance consistent with the measured cosmological parameter Ω_{Planck} on the left part of the graphs. These points correspond to the Higgs resonance on the scattering cross section, and are always present in the model. Again, as Higgs mediated interactions are almost completely ruled out and E_e interactions with the Higgs boson are strongly suppressed, we are not interested in their analysis in this work.

So, from Fig. 4, we can see that the dominant portal for the interactions of E_e is the Z' portal, as the red bands giving the relic abundance consistent with Planck results [4] are placed symmetrically about the black line with equation $M_{E_e} = M_{Z'}/2$, indicating a resonance for every value of $M_{Z'}$ shown in the figure. This conclusion is consistent with the analysis of Ref. [69], which found constraints on the Z' boson mass using bounds obtained from direct detection experiments, and requires no fine-tuning on the parameters of the model.

VI. CONSTRAINTS ON THE MASS OF THE Z' BOSON AND THE v_χ VEV USING DM DIRECT DETECTION EXPERIMENTS

Now that we have identified the dominant portal, we proceed to the determination of constraints on the properties of our DM candidate coming from the XENON1T direct detection experiment [16], and the future sensitivity of the LZ experiment [17]. In order to do so, we need to identify the parameters of the 3 − 3 − 1 model corresponding to quantities entering in Eq. (3), calculated in terms of the simplified models described by the Lagrangian in (2). It is worth mentioning here the difference of this work, where the DM candidate is a fermion with interactions mediated by a gauge boson, with previous analyses in terms of simplified models, as for example the ones in [21–23], where the DM particle is a scalar, with interactions through the Higgs portal or the exchange of fermions or scalars not included in the SM.

The terms in the Lagrangian of the 3 − 3 − 1 model which correspond to interactions of E_e with the vector mediator Z', in the form given in Eq. (2), can be written as

$$\mathcal{L}_{331} \supset c_1 \overline{E_e}\gamma^\mu(1-\gamma^5)E_e Z'_\mu + c_2 \bar{u}\gamma^\mu(c_3+\gamma^5)uZ'_\mu + c_4 \bar{d}\gamma^\mu(c_5+c_6\gamma^5)dZ'_\mu, \tag{43}$$

where the constants c_i, $i = 1, \ldots, 6$, are coefficients depending on the specific parameters of the model, and are given by

$$\begin{aligned} c_1 &= \frac{e(1-s_W^2)}{2c_W s_W\sqrt{3-4s_W^2}}, \\ c_2 &= \frac{1}{2(1-s_W^2)}c_1, \\ c_3 &= -1+\frac{8}{3}s_W^2, \\ c_4 &= -\frac{1}{3}c_2, \\ c_5 &= 2s_W^2 + [(V_{1,1}^{\mathrm{CKM}})^2 + (V_{2,1}^{\mathrm{CKM}})^2](3-4s_W^2) \\ &\quad - (V_{3,1}^{\mathrm{CKM}})^2(3-2s_W^2), \\ c_6 &= 4s_W^2 - c_5, \end{aligned} \tag{44}$$

where e, s_W, and c_W were defined in Sec. IV, and $V_{i,j}^{\mathrm{CKM}}$ are the i, j components of the Cabibbo-Kobayashi-Maskawa (CKM) matrix of the quark fields.

Taking these considerations into account, we can make the following identification of the parameters in (2):

$$g = c_1, \tag{45}$$

$$V_{E_e}^{Z'} = 1, \qquad A_{E_e}^{Z'} = 1, \tag{46}$$

$$V_u^{Z'} = \frac{c_2 c_3}{c_1}, \qquad A_u^{Z'} = -\frac{c_2}{c_1}, \tag{47}$$

$$V_d^{Z'} = \frac{c_4 c_5}{c_1}, \qquad A_d^{Z'} = -\frac{c_4 c_6}{c_1}, \tag{48}$$

where we have replaced the indices for the DM candidate (ψ), the mediator (U_μ), and the SM fermion (f) in Eq. (2) for the corresponding particle names in the 3 − 3 − 1 model, E_e, Z'_μ and u, d, respectively.

With this identification, we can proceed to the calculation of the spin-independent scattering cross section with protons, in order to set constraints on the masses of the DM candidate E_e and the vector mediator Z'. In order to do this, we have calculated σ_p^{SI} in two different situations: as given by Eq. (3) (which we will call $\sigma_p^{Z'}$ from now on), which assumes that E_e interactions are mediated only by Z' and there are no other particles in the physical spectrum (besides SM particles), and considering the full particle content of the 3 − 3 − 1 model (henceforth called σ_p^{331}), with all its possible portals, as done by the micrOMEGAs package [67].

When performing this calculation, we have found that the value of $\sigma_p^{Z'}$ is always greater than σ_p^{331} by a fixed factor of approximately 1.339. This factor comes from neglecting the other contributing diagrams in the scattering cross section of E_e with quarks, which produce a destructive interference with the diagram mediated by Z', in all the parameter space scanned in this work. So, in order to take into account this difference and be able to compare the results of the full 3 − 3 − 1 model with the predictions of simplified models, we have included a normalization factor in Eq. (3).[2]

In Fig. 5 we show the constraints on the E_e and Z' masses set by an extrapolation of the data from the XENON1T direct detection experiment [16] (orange region), and the future weakly interacting massive particle sensitivity of the LZ experiment [17] (green), where the red points have a relic density consistent with that measured by Planck [4], and the vertical dashed blue lines correspond to the favored region obtained from the contributions of new particles in the 3 − 3 − 1 model to the anomalous magnetic moment of the muon, as shown in Fig. 2, with $M_{Z'}$ calculated using Eq. (42).

From Fig. 5, we can see that the measured value of DM relic abundance can be accomplished in two different regimes: the one dominated by the Z'_μ resonance, characterized by the red lines labeled (I) and (II) in the figure and placed symmetrically about the resonant condition $M_{E_e} = M_{Z'/2}$, and the degenerate regime, when the mass of the DM candidate is very close to the mass of the $Y^\pm$ gauge boson in the same discrete group which makes E_e stable,

[2]In our numerical calculations, we have found the ratio $\sigma_p^{331}/\sigma_p^{Z'} = 0.746846$, with a standard deviation 1.5×10^{-5}, calculated over a sample with approximately 10^6 data of σ_p^{331} and $\sigma_p^{Z'}$, calculated simultaneously.

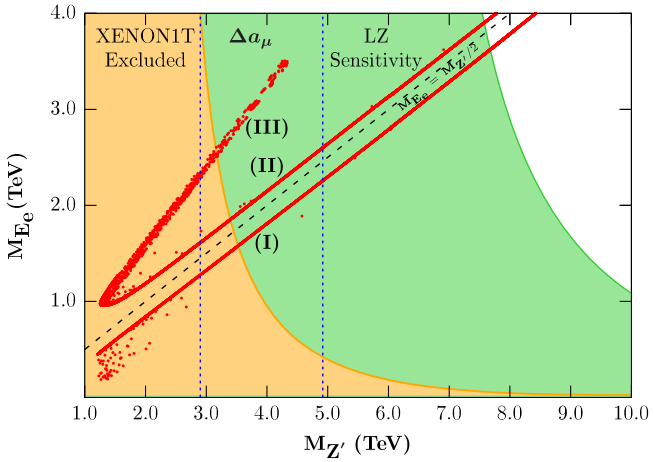

FIG. 5. Constraints on E_e and Z' masses set by XENON1T [16], and the future sensitivity of the LZ experiment [17]. All red points have a relic abundance in the interval measured by the Planck Collaboration [4], and the vertical dashed blue lines correspond to the favored region by the contribution of new particles to the anomalous magnetic moment of the muon. The red lines labeled (I) and (II) correspond to the Z' resonance on the DM abundance, and the line (III) corresponds to an enhancement on the relic abundance due to the degenerate mass regime, where $M_{E_e} \sim M_Y$.

labeled as (III) in Fig. 5. It is important to note here that this last regime requires some fine-tuning in the parameters of the model, in order to reach a degenerate mass scenario, $M_{E_e} \approx M_Y$.

Also from this figure we observe that, in order to make the $3-3-1$ model a suitable framework including fermion DM, there will be minimum values of M_{E_e} and $M_{Z'}$ which satisfy the constraints on the DM relic density and spin-independent scattering cross section with protons. Due to the direct dependence of the Z' mass on v_χ given by Eq. (42), the minimum values of the boson mass can be translated to constraints on the $SU(3)_L$ symmetry breaking scale, on which all masses of new particles are strongly dependent. The minimum values of the masses and the symmetry breaking scale, for each of the bands in Fig. 5, are shown in Table I, which shows the exclusion limits set by the two different direct detection experiments considered.

The minimum values of $M_{Z'}$ are higher than the ones presented in Ref. [70], where the authors extended the analysis of decays of a new gauge boson to dilepton final states performed in [71] to impose constraints on models with an additional particle of this type, in order to find lower bounds on the mass of the Z' boson of the $3-3-1$ model. On the other hand, our bounds on $M_{Z'}$ are consistent with the results of Ref. [72], which analyze LHC data on flavor changing neutral currents and dilepton resonance searches.

Finally, the favored window for the contribution of new particles in the model to Δa_μ, giving the boundaries on v_χ shown in Eq. (41), sets the following minimum and maximum values for the mass of the Z' gauge boson when we use Eq. (42):

$$2.9\ \text{TeV} \lesssim M_{Z'} \lesssim 4.9\ \text{TeV} \quad (95\%\ \text{C.L.}), \tag{49}$$

which, when combined with the constraints found with the results of the XENON1T [16] direct detection experiment gives a narrower window for the mass of this new gauge boson, with the same lower bounds shown in Table I and an upper bound given by the maximum value in Eq. (49). It is interesting to note that the minimum values of v_χ obtained here are consistent with the ones obtained through the analysis of vacuum stability of the scalar potential and the constraints on the mass of new particles developed in [55], even though the fermion content of the models is different. On the other hand, with the comparison of the favored region represented by the vertical dashed blue lines in Fig. 5 and the constraint of the future sensitivity of the LZ experiment [17], we can set constraints on the highest energy scale of the $3-3-1$ model with heavy neutral leptons as a suitable framework with a fermion candidate to DM, taking the additional constraint of the $(g-2)_\mu$ anomaly into account.

VII. SUMMARY OF CONSTRAINTS

To summarize all constraints on the mass of the Z' boson or the highest VEV of the $3-3-1$ model, we have constructed Fig. 6, where the horizontal bars indicate the excluded regions for $M_{Z'}$ and v_χ, related by the expression given in Eq. (42), as obtained from different analyses. The

TABLE I. Minimum Z' and lepton E_e masses required for the $3-3-1$ model with heavy neutral leptons give a relic E_e density consistent with Planck [4], and evading the limits set by XENON1T [16] and the future sensitivity of LZ [17], for the scenarios denoted, respectively, as (I), (II), and (III) in Fig. 5.

Experiment	Regime	$M_{E_e}^{\min}$ (TeV)	$M_{Z'}^{\min}$ (TeV)	$v_\chi^{\min}$ (TeV)
XENON1T	Lower resonance (I)	1.6	3.6	8.8
	Upper resonance (II)	1.9	3.4	8.4
	Degenerate region (III)	2.6	3.2	7.9
LZ	Lower resonance (I)	3.6	7.7	19
	Upper resonance (II)	3.9	7.6	19

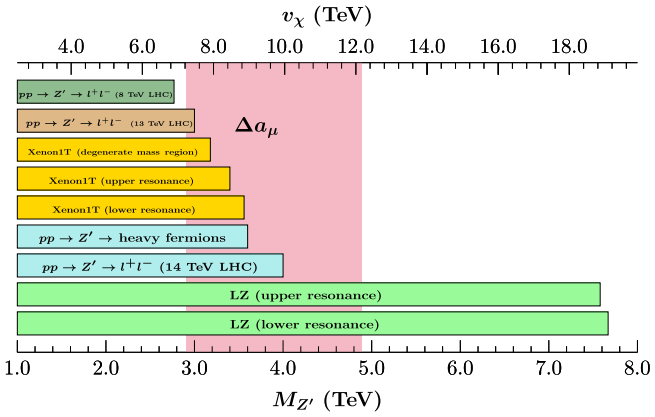

FIG. 6. Excluded values for the Z' boson mass and the v_χ VEV set by different analyses: Z' decaying to dilepton final states in pp collisions using data from LHC at a center-of-mass energy of 8 TeV (dark green) [70] and 13 TeV (brown) [72], the exclusion limits set on this work (yellow bars) for the spin-independent cross section of fermion DM using XENON1T results [16], the negative results of dilepton searches at the 14 TeV LHC, both to heavy ($M \sim 1$ TeV) and SM fermions (cyan) [56] and, finally, the constraints set on this work (light green) using the future sensitivity of the LZ experiment [17]. The shaded vertical region shows the favored values (95% C.L.) of v_χ and $M_{Z'}$ obtained from the analysis of the contributions of new particles in the $3-3-1$ model with heavy neutral fermions to the anomalous magnetic moment of the muon.

shaded vertical region in Fig. 6 gives the favored values (95% C.L.) of v_χ calculated from the total contribution of new physical states of the $3-3-1$ model considered in this work to the anomalous magnetic moment of the muon, Δa_μ. In this graph, the green and brown bars show the analyses of the process $pp \to Z' \to l^+l^-$ using LHC data at 8 [70] and 13 TeV [72], the yellow bars show the constraints set by the comparison of DM in the $3-3-1$ model with the predictions of simplified models, as performed in this work, the cyan bars, giving the current strongest constraints, show the bounds obtained by the decay of Z' to heavy and light fermions in the 14 TeV LHC [56] and, finally, the light green bars show the bounds obtained from the future sensitivity of the LZ direct detection experiment [17], obtained in this work.

It is important to remark here that the projected sensitivity of the LZ experiment has the potential to rule out Z' masses below 7.6 TeV, as shown in Table I, and this result, combined with the favored window for Δa_μ shown by the vertical shaded region in Fig. 6, could rule out the $3-3-1$ model with a neutral fermion candidate to DM as a suitable extension of the SM.

VIII. CONCLUSIONS

In this work we have found constraints on a $3-3-1$ model, with a heavy neutral fermion as a DM candidate, coming from three different experimentally measured quantities: the anomalous magnetic moment of the muon, the DM relic density and the spin-independent scattering cross section of DM with protons.

In order to do this, we have calculated the contribution of new particles to the correction Δa_μ to the anomalous magnetic moment of the muon, finding a favored window for the $SU(3)_L$ symmetry breaking scale of the model, namely 7.2 TeV $\lesssim v_\chi \lesssim$ 12.2 TeV. The importance of this symmetry breaking scale lies on the strong dependence of all masses of new particles in the model with this quantity.

On the other hand, considering a fermion DM candidate in the model with a relic density consistent with cosmological observations, and from the analysis of the spin-independent scattering cross section of this candidate with protons (σ_p), we were able to find minimum values of this symmetry breaking scale due to its relation with the mass of the vector portal of DM-SM interaction, a neutral gauge boson Z'_μ.

In order to identify this particle as the dominant portal, we have made a comparison of the values of σ_p^{331}, the exact value of σ_p considering all particles and interactions in the $3-3-1$ model, and $\sigma_p^{Z'}$, the DM-proton scattering cross section calculated from a comparison of the $3-3-1$ model with the predictions of simplified models for DM interactions.

The comparison of the $3-3-1$ model predictions for the DM relic density and the spin-independent scattering cross section with the measurements of the Planck [4] and XENON1T [16] collaborations, and the combination with the favored window coming from the measurement of the anomalous magnetic moment of the muon [15] lead to the bounds $v_\chi^{\min} \lesssim v_\chi \lesssim 12.2$ TeV and $M_{Z'}^{\min} \lesssim M_{Z'} \lesssim 4.9$ TeV for the $SU(3)_L$ symmetry breaking scale and the Z'_μ boson mass, respectively, where the values of $v_\chi^{\min}$ and $M_{Z'}^{\min}$ depend on the regime associated with the production of fermion DM in the model, and are of order 8–9 TeV and 3–4 TeV, respectively.

Finally, the comparison of the favored region for Δa_μ with the future sensitivity of the LZ direct detection experiment [17], ruling out values of v_χ less than ∼19 TeV and values of $M_{Z'}$ lower than 7.5 TeV, leads to the conclusion that the $3-3-1$ model with heavy neutral fermions can not be a suitable extension of the SM when the DM candidate in the model corresponds to the heavy neutral fermion of the electron flavor. In this case, other neutral particles being odd under the same discrete symmetry stabilizing DM, such as a scalar or a gauge boson in the physical spectrum, could give different results.

ACKNOWLEDGMENTS

C. E. A. S. is grateful for the support of CNPq, under Grant No. 159237/2015-7 during his stay at IFGW/UNICAMP. O. L. G. P. is grateful for the support of FAPESP funding Grant No. 2014/19164-6, CNPq

research fellowships 307269/2013-2, 304715/2016-6, and 306565/2019-6, and for partial support from FAEPEX funding Grant No. 3162/18. This study was financed in part by the Coordenação de Aperfeiçoamento de Pessoal de Nível Superior–Brasil (CAPES), Finance Code 001.

[1] Y. Fukuda *et al.* (Super-Kamiokande Collaboration), Phys. Rev. Lett. **81**, 1562 (1998).
[2] F. Jegerlehner and A. Nyffeler, Phys. Rep. **477**, 1 (2009).
[3] R. Cooke, M. Pettini, R. A. Jorgenson, M. T. Murphy, and C. C. Steidel, Astrophys. J. **781**, 31 (2014).
[4] N. Aghanim and *et al.* (Planck Collaboration), Astron. Astrophys. **641**, A6 (2020).
[5] L. Bergström, Rep. Prog. Phys. **63**, 793 (2000).
[6] G. Bertone, D. Hooper, and J. Silk, Phys. Rep. **405**, 279 (2005).
[7] N. Aghanim *et al.* (Planck Collaboration), Astron. Astrophys. **641**, A1 (2020).
[8] A. L. Fitzpatrick, W. Haxton, E. Katz, N. Lubbers, and Y. Xu, J. Cosmol. Astropart. Phys. 02 (2013) 004.
[9] J. Abdallah *et al.*, Phys. Dark Universe **9–10**, 8 (2015).
[10] A. DiFranzo, K. I. Nagao, A. Rajaraman, and T. M. P. Tait, J. High Energy Phys. 11 (**2013**) 014; 01 (2014) 162(E).
[11] A. Berlin, D. Hooper, and S. D. McDermott, Phys. Rev. D **89**, 115022 (2014).
[12] D. Alves (LHC New Physics Working Group), J. Phys. G **39**, 105005 (2012).
[13] L. Roszkowski, E. M. Sessolo, and S. Trojanowski, Rep. Prog. Phys. **81**, 066201 (2018).
[14] J. L. Feng *et al.*, in *Proceedings of the 2013 Community Summer Study on the Future of U.S. Particle Physics: Snowmass on the Mississippi (CSS2013): Minneapolis, MN, 2013*, pp. 127–183 [arXiv:1401.6085].
[15] G. W. Bennett *et al.* (Muon g-2 Collaboration), Phys. Rev. D **73**, 072003 (2006).
[16] E. Aprile *et al.* (XENON Collaboration), Phys. Rev. Lett. **119**, 181301 (2017).
[17] D. Akerib *et al.* (LUX-ZEPLIN Collaboration), Phys. Rev. D **101**, 052002 (2020).
[18] C. E. Alvarez-Salazar, O. L. G. Peres, and B. L. Sánchez-Vega, Astron. Nachr. **340**, 135 (2019).
[19] C. Kelso, H. N. Long, R. Martinez, and F. S. Queiroz, Phys. Rev. D **90**, 113011 (2014).
[20] J. K. Mizukoshi, C. A. de S. Pires, F. S. Queiroz, and P. S. Rodrigues da Silva, Phys. Rev. D **83**, 065024 (2011).
[21] L. Calibbi, R. Ziegler, and J. Zupan, J. High Energy Phys. 07 (2018) 046.
[22] K. Kowalska and E. M. Sessolo, J. High Energy Phys. 09 (2017) 112.
[23] E. M. Sessolo and K. Kowalska, Proc. Sci., EPS-HEP2017 (**2017**) 338.
[24] P. Langacker, *The Standard Model and Beyond* (CRC Press, Boca Raton, FL, 2017).
[25] A. Buras, J. R. Ellis, M. Gaillard, and D. V. Nanopoulos, Nucl. Phys. **B135**, 66 (1978).
[26] J. R. Ellis, D. V. Nanopoulos, and K. Tamvakis, Phys. Lett. **121B**, 123 (1983).
[27] J. H. Schwarz, Phys. Rep. **89**, 223 (1982).
[28] D. Ida, J. High Energy Phys. 09 (2000) 014.
[29] S. P. Martin, in *Perspectives on Supersymmetry II* (World Scientific, Singapore, 2010), pp. 1–153.
[30] M. Schmaltz and D. Tucker-Smith, Annu. Rev. Nucl. Part. Sci. **55**, 229 (2005).
[31] T. Han, H. E. Logan, B. McElrath, and L.-T. Wang, Phys. Rev. D **67**, 095004 (2003).
[32] W. A. Bardeen, C. T. Hill, and M. Lindner, Phys. Rev. D **41**, 1647 (1990).
[33] Z. Chacko and A. E. Nelson, Phys. Rev. D **62**, 085006 (2000).
[34] N. Arkani-Hamed, L. J. Hall, D. Tucker-Smith, and N. Weiner, Phys. Rev. D **62**, 105002 (2000).
[35] T. R. Slatyer, Phys. Rev. D **93**, 023527 (2016).
[36] *Anticipating The Next Discoveries In Particle Physics*, edited by R. Essig and I. Low (World Scientific, Boulder, 2018), https://doi.org/10.1142/10798.
[37] M. Klasen, M. Pohl, and G. Sigl, Prog. Part. Nucl. Phys. **85**, 1 (2015).
[38] G. Arcadi, M. Dutra, P. Ghosh, M. Lindner, Y. Mambrini, M. Pierre, S. Profumo, and F. S. Queiroz, Eur. Phys. J. C **78**, 203 (2018).
[39] M. Singer, J. W. F. Valle, and J. Schechter, Phys. Rev. D **22**, 738 (1980).
[40] F. Pisano and V. Pleitez, Phys. Rev. D **46**, 410 (1992).
[41] P. H. Frampton, Phys. Rev. Lett. **69**, 2889 (1992).
[42] J. C. Montero, F. Pisano, and V. Pleitez, Phys. Rev. D **47**, 2918 (1993).
[43] R. Foot, O. F. Hernandez, F. Pisano, and V. Pleitez, Phys. Rev. D **47**, 4158 (1993).
[44] R. Foot, H. N. Long, and T. A. Tran, Phys. Rev. D **50**, R34 (1994).
[45] B. L. Sánchez-Vega, E. R. Schmitz, and J. C. Montero, Eur. Phys. J. C **78**, 166 (2018).
[46] P. V. Dong and H. N. Long, Int. J. Mod. Phys. A **21**, 6677 (2006).
[47] P. V. Dong, H. N. Long, and D. V. Soa, Phys. Rev. D **75**, 073006 (2007).
[48] A. G. Dias, J. Leite, D. D. Lopes, and C. C. Nishi, Phys. Rev. D **98**, 115017 (2018).
[49] A. G. Dias, V. Pleitez, and M. D. Tonasse, Phys. Rev. D **67**, 095008 (2003).
[50] J. C. Montero, A. Romero, and B. L. Sánchez-Vega, Phys. Rev. D **97**, 063015 (2018).
[51] A. R. Romero Castellanos, C. E. Alvarez-Salazar, and B. L. Sánchez-Vega, Astron. Nachr. **340**, 131 (2019).
[52] P. V. Dong, D. T. Huong, F. S. Queiroz, and N. T. Thuy, Phys. Rev. D **90**, 075021 (2014).

[53] R. A. Diaz, R. Martinez, and F. Ochoa, Phys. Rev. D **72**, 035018 (2005).
[54] A. J. Buras, F. De Fazio, J. Girrbach, and M. V. Carlucci, J. High Energy Phys. 02 (**2013**) 023.
[55] B. L. Sánchez-Vega, G. Gambini, and C. E. Alvarez-Salazar, Eur. Phys. J. C. **79**, 299 (2019).
[56] Q.-H. Cao and D.-M. Zhang, arXiv:1611.09337.
[57] P. Lancaster and M. Tismenetsky, *The Theory of Matrices: With Applications* (Elsevier, San Diego, CA, 1985).
[58] B. J. McCartin, *Rayleigh-Schrödinger Perturbation Theory: Pseudoinverse Formulation* (Hikari Limited, Bulgaria, 2009).
[59] A. Czarnecki and W. J. Marciano, Phys. Rev. D **64**, 013014 (2001).
[60] F. S. Queiroz and W. Shepherd, Phys. Rev. D **89**, 095024 (2014).
[61] M. Tanabashi *et al.* (Particle Data Group), Phys. Rev. D **98**, 030001 (2018).
[62] C. Kelso, P. R. D. Pinheiro, F. S. Queiroz, and W. Shepherd, Eur. Phys. J. C **74**, 2808 (2014).
[63] N. D. Christensen and C. Duhr, Comput. Phys. Commun. **180**, 1614 (2009).
[64] A. Alloul, N. D. Christensen, C. Degrande, C. Duhr, and B. Fuks, Comput. Phys. Commun. **185**, 2250 (2014).
[65] A. Belyaev, N. D. Christensen, and A. Pukhov, Comput. Phys. Commun. **184**, 1729 (2013).
[66] M. Escudero, A. Berlin, D. Hooper, and M.-X. Lin, J. Cosmol. Astropart. Phys. 12 (**2016**) 029.
[67] D. Barducci, G. Belanger, J. Bernon, F. Boudjema, J. Da Silva, S. Kraml, U. Laa, and A. Pukhov, Comput. Phys. Commun. **222**, 327 (2018).
[68] K. Griest and D. Seckel, Phys. Rev. D **43**, 3191 (1991).
[69] S. Profumo and F. S. Queiroz, Eur. Phys. J. C **74**, 2960 (2014).
[70] C. Salazar, R. H. Benavides, W. A. Ponce, and E. Rojas, J. High Energy Phys. 07 (**2015**) 096.
[71] G. Aad *et al.* (ATLAS Collaboration), Phys. Rev. D **90**, 052005 (2014).
[72] F. S. Queiroz, C. Siqueira, and J. W. F. Valle, Phys. Lett. B **763**, 269 (2016).